

## **Analytical Solution of Suspended Sediment Concentration Profile: Relevance of Dispersive Flow Term in Vegetated Channels**

Item Type	Article
Authors	Huai, W.;Yang, L.;Guo, Yakun
Citation	Huai W, Yang L and Guo Y (2020) Analytical Solution of Suspended Sediment Concentration Profile: Relevance of Dispersive Flow Term in Vegetated Channels. Water Resources Research. 56(7): e2019WR027012.
DOI	<a href="https://doi.org/10.1029/2019WR027012">https://doi.org/10.1029/2019WR027012</a>
Rights	(c) 2020 AGU. Full-text reproduced in accordance with the publisher self-archiving policy.
Download date	2025-06-16 21:34:45
Link to Item	<a href="http://hdl.handle.net/10454/17958">http://hdl.handle.net/10454/17958</a>

Analytical Solution of Suspended Sediment Concentration Profile: Relevance of  
Dispersive Flow Term in Vegetated Channels

Wenxin Huai<sup>1</sup>, Liu Yang<sup>1</sup>, and Yakun Guo<sup>2</sup>

<sup>1</sup> State Key Laboratory of Water Resources and Hydropower Engineering Science, Wuhan  
University, Wuhan, Hubei 430072, China.

<sup>2</sup> Faculty of Engineering & Informatics, University of Bradford, BD7 1DP, UK.

Corresponding author: Wenxin Huai ([wxhuai@whu.edu.cn](mailto:wxhuai@whu.edu.cn))

**Key Points:**

- A dispersive model is proposed to investigate the sediment transport in the vegetated open channels with parameters fitted with experiments.
- Analytical solution of the vertical suspended sediment concentration profile is derived for submerged and emergent vegetated open channels.
- The effects of dispersion on suspended sediment concentration in the vegetated channels is demonstrated by the double-averaging method.

## Abstract

Simulation of the suspended sediment concentration (SSC) has great significance in predicting the sediment transport rate, vegetation growth and the river ecosystem in the vegetated open channel flows. The present study focuses on investigating the vertical SSC profile in the vegetated open channel flows. To this end, a model of the dispersive flux is proposed in which the dispersive coefficient is expressed as partitioned linear profile above or below the half height of vegetation. The double-averaging method, i.e. time-spatial average, is applied to improve the prediction accuracy of the vertical SSC profile in the vegetated open channel flows. The analytical solution of SSC in both the submerged and the emergent vegetated open channel flows is obtained by solving the vertical double-averaging sediment advection-diffusion equation. The morphological coefficient, a key factor of the dispersive coefficient, is obtained by fitting the existing experimental data. The analytically predicted SSC agrees well with the experimental measurements, indicating that the proposed model can be used to accurately predict the SSC in the vegetated open channel flows. Results show that the dispersive term can be ignored in the region without vegetation, while the dispersive term has significant effect on the vertical SSC profile within the region of vegetation. The present study demonstrates that the dispersive coefficient is closely related to the vegetation density, the vegetation structure and the stem Reynolds number, but has little relation to the flow depth. With a few exceptions, the absolute value of the dispersive coefficient decreases with the increase of the vegetation density and increases with the increase of the stem Reynolds number in the submerged vegetated open channel flows.

## Keywords

Suspended sediment concentration; Double-averaging method; Dispersive flow; Vegetated open channel flows;

## 1 Introduction

Aquatic vegetation in the vegetated open channel flows can significantly affect flow velocity and turbulence structure and momentum exchange processes (Huai et al., 2009a; Nepf, 2012; Li et al., 2015; Li et al., 2019) as well as the sediment transport (Le Bouteiller & Venditti, 2015; Li & Katul, 2019; Yang & Nepf, 2019). Previous studies (Wang et al., 2016; Li et al., 2018) showed that the vertical profile of suspended sediment concentration (referred as SSC hereafter), an important characteristic for waterway ecosystem, is much more complicated in the vegetated open channels than that in channels without vegetation, due to the great variation of the turbulent strength in the vertical direction. Studies of Kim et al. (2018) and Västilä and Järvelä (2018) on the suspended sediment deposition within and around a circular vegetation patch showed that the vegetation enhanced the deposition of sediment in the vegetation region. These studies showed that aquatic vegetation greatly affects the sediment transport rate. The previously dominant methodologies of simulating the suspended sediment transport are based on the time-averaging Navier-Stokes equations or advection-diffusion equations, including turbulent diffusion model (Li et al., 2018; Kundu, 2019), two-phase flow model (Fu et al., 2005) and flume experimental model (Kim et al., 2018; Västilä & Järvelä, 2018). In the vegetated open channels, the spatial heterogeneity of flow field is significantly enhanced by the presence of aquatic vegetation. In order to improve the simulation accuracy in the vegetated open channel flows, the

double-averaging methodology is introduced to extend the time averaging flow field to time-spatial averaging field (Nikora et al., 2007a; Wang et al., 2014).

The double-averaging method is usually applied to the large eddy simulation (LES), direct numerical simulation (DNS) and physical model to study the spatial heterogeneity in the open channel flow and airflow. To investigate the impact of heterogeneity on edge-flow dynamics, Boudreault et al. (2017) applied double-averaging method to the LES to simulate the forest-edge flows. Their results showed that the forest heterogeneity facilitated flow penetration into the vegetation (i.e. trees and plants). In the roughness region, e.g. rough bed, the heterogeneity is strong. Stoesser and Nikora (2008) and Han et al. (2017) applied the LES with the double-averaging method to evaluate the effect of the roughness on the rough-bed flows. In addition, Coceal et al. (2006, 2007, 2008) used the regular arrays of cubical obstacles as the rough-bed to study the turbulent flow and the dispersive stress in roughness flows with the DNS and the double-averaging method. Laboratory experiment is another methodology to study the flow with spatial heterogeneity. Poggi and Katul (2008a) and Moltchanov et al. (2015) carried out flume experiments to investigate the effect of the spatial heterogeneity on the flow structure in the vegetated open channel flows, while Spiller et al. (2015) conducted flume experiments to examine the role of the heterogeneity in non-uniform steady and unsteady flow over a rough bed. These numerical and experimental studies showed that the double-averaging method can reduce the inconvenience of time-averaging variables in volume resulted from the spatial heterogeneity. In addition, the dispersive flux (or stress), an additional key term in the double-averaging method, is generated due to the deviation of time averaging field from space averaging field (Tanino & Nepf, 2008a).

So far the dispersive term in the vegetated open channels has been poorly defined, making it difficult to clearly express the dispersive stress. Florens et al. (2013) conducted laboratory experiments and measured the fluctuation velocity using particle image velocimetry (PIV) to investigate the dispersive stress in the vegetated open channel flows. Poggi et al. (2004a, 2004b) and Poggi and Katul (2008b) conducted flume experiments with the submerged vegetation made of rigid cylindrical rods. They found that the maximum value of the dispersive stress had comparable magnitude (almost 30% of the total stress) with the Reynolds stress (almost 70% of the total stress) within the vegetation region for sparse vegetated flow and was trivial for dense vegetated flow. They also found that the dispersive stress appeared to decrease with the increase of vegetation density. Righetti (2008) conducted experiment with the natural vegetation (*salix pentandra*) and showed that the dispersive stress was large and could not be ignored in natural flexible vegetated flow. These experimental studies revealed that (i) the dispersive stress was significant within the vegetation region, insignificant in the region without vegetation; and (ii) the value of the dispersive stress reached the maximum value at the position close to the half height of vegetation and gradually decreased toward both the channel bottom and the water surface. In addition, the dispersive stress is not only significant in the vegetated flow, but also in the rough-bed flow (Nikora et al., 2007b). The study of Nikora et al. (2007b) for the flow over a rough-bed showed that the double-averaging method could identify the specific flow layers and flow types and the dispersive stress existed in the roughness region of the rough-bed flow.

Most previous studies only focused on the phenomenon of the dispersive stress. To the authors' best knowledge, so far little knowledge exists about the effect of the dispersive flux on the vertical SSC profile, the application of the dispersive term on the mass transport and the

model of the dispersive coefficient. This motivates this study, which focuses on developing a new dispersive coefficient model and investigating the relationship of dispersive strength with canopy density and the vertical SSC profile in the steady vegetated open channel flows. Recently, Tai and Huang (2019) simulated the suspended sediment transport with the stochastic Lagrangian model. However, their simulated vertical SSC profile was inconsistent with the experimental observations (see Figure 11 in the literature of Tai and Huang (2019)). Huai et al. (2019) took dispersion into account and applied the random displacement model, also a Lagrangian model, to simulate the vertical SSC profile in the vegetated open channel flows. Though their simulated results were almost consistent with the experimental observations, some deviation still existed in the region of vegetation for the submerged vegetated open channel flow. The reason for this deviation in the vegetation region may be due to the hypothesis that the profile of the dispersive coefficient was the same as the turbulent diffusion coefficient with different magnitude. This could mean that the distribution of the dispersive coefficient is different from the turbulent diffusion coefficient in the vegetated open channel flows. Yuuki and Okabe (2002) used the dispersive coefficient, the averaged longitudinal flow velocity of cross-section and the averaged SSC of cross-section to model the dispersive flux. As discussed above, the comparable magnitude of dispersion only exists in the vegetation region and the local SSC differs from the averaged SSC of cross-section. Therefore, from the point of view of the physical mechanism, it will be much better to use the local SSC to scale the dispersive flux. In order to improve the simulation of the vertical SSC profile, in this study, the double-averaging method is thus applied to investigate the sediment transport in the vegetated open channel flows by assuming that the dispersive term only exists in the vegetation region. In order to reduce the deviation caused by the application of the averaged SSC of cross-section, a new approximation approach is then proposed in this study to express the dispersive flux of suspended sediment, where the dispersive flux is proportional to the local SSC in the vegetated open channel flows. The analytical solution of the vertical SSC profile is obtained by solving the double-averaging advection-diffusion equations, which are influenced by vegetation density, vegetation structure, flow characteristics and the spatial arrangement of vegetation.

## 2 Theory

### 2.1 Double-averaging Method

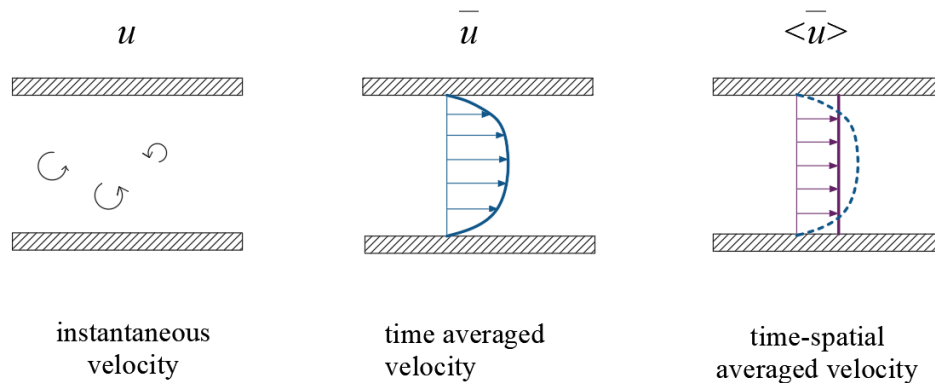


**Figure 1.** The schematic diagram of time-spatial averaging method for platforms flow.

Though the double-averaging method can be found in previous studies (e.g. Nikora et al., 2007a, b), we present a brief description for convenience and completeness. To this end, the flow between the platforms, as shown in Figure 1, is taken as an example to demonstrate the concept of the double-averaging method. The instantaneous longitudinal flow velocity (denoted as  $u$ ) can be decomposed as  $u = \bar{u} + u'$  based on the Reynold's decomposition approach, while the time-averaging velocity can be further decomposed as  $\bar{u} = \langle \bar{u} \rangle + u''$ . In these decompositions, the overbar denotes the time averaged variables, the single prime represents the fluctuation velocity, i.e. the deviation of instantaneous variables from the time-averaging variables, the double primes denotes the time averaged deviations from spatial averaged variables and the symbol  $\langle \rangle$  represents the spatially averaged variables. Instantaneous velocity, therefore, can be expressed as  $u = \langle \bar{u} \rangle + u'' + u'$  in the time-spatial averaging flow field. This means that the double-averaging method includes two main steps: (1) firstly applying time averaging to the equations for instantaneous variables; (2) secondly applying the spatial averaging to the equations which have already been averaged in the time domain.

Though the double-averaging method has been widely applied to investigate the flow field in rough open channel and river flow, the method has been hardly ever applied to estimate the vertical SSC profile in the vegetated open channel flows. In this paper, the authors will propose a new model for describing the dispersion in sediment-laden flow with vegetation and apply the double-averaging method to calculate the vertical SSC profile. The instantaneous advection-diffusion equation of sediment is written as following based on the mass conservation:

$$\frac{\partial c}{\partial t} + \frac{\partial(u_j c)}{\partial x_j} - \frac{\partial}{\partial x_j} \left( K_m \frac{\partial c}{\partial x_j} \right) + S = 0 \quad (1)$$

where  $t$  represents time,  $c$  is the instantaneous SSC,  $x_j$  is the  $j$ th direction ( $x_1 = x$  represents the longitudinal direction;  $x_2 = y$  represents the transverse direction;  $x_3 = z$  represents the vertical direction),  $u_j$  ( $j=1, 2$  and  $3$ ) is the instantaneous flow velocity component in the directions of  $x$ ,  $y$  and  $z$ , respectively;  $K_m$  represents the molecular diffusion coefficient and  $S$  represents the source or sink of sediment. The first term in Equation (1) is the variation of SSC with time, the second term represents the transport of sediment advection flux in the  $x_j$  direction and the third term is the transport of sediment molecular diffusion flux.

Applying the double-averaging approach by inserting the decomposed instantaneous variables of  $c$ ,  $u_j$  and  $S$  as  $\varphi = \bar{\varphi} + \varphi'$  (where  $\varphi$  represents the variables) into Equation (1) yields:

$$\frac{\partial}{\partial t} (\bar{c} + c') + \frac{\partial}{\partial x_j} [(\bar{u}_j + u_j')(\bar{c} + c')] - \frac{\partial}{\partial x_j} \left( K_m \frac{\partial (\bar{c} + c')}{\partial x_j} \right) + \bar{S} + S' = 0 \quad (2)$$

Applying time-averaging to Equation (2) yields:

$$\frac{\partial}{\partial t} (\overline{\bar{c} + c'}) + \frac{\partial}{\partial x_j} [(\overline{\bar{u}_j + u_j'}) (\overline{\bar{c} + c'})] - \frac{\partial}{\partial x_j} \left( \overline{K_m \frac{\partial (\bar{c} + c')}{\partial x_j}} \right) + \bar{S} + \bar{S}' = 0 \quad (3)$$

According to the rules:  $\overline{f + \varphi} = \overline{f} + \overline{\varphi}$ ,  $\overline{\sigma f} = \sigma \overline{f}$  and  $\overline{f'} = 0$  (where  $f$  represents a variable and  $\sigma$  is a constant), Equation (3) can be simplified as (Tanino & Nepf, 2008a; Termini, 2019):

$$\frac{\partial \bar{c}}{\partial t} + \frac{\partial}{\partial x_j} (\bar{u}_j \bar{c} + \overline{u_j' c'}) - \frac{\partial}{\partial x_j} \left( K_m \frac{\partial \bar{c}}{\partial x_j} \right) + \bar{S} = 0 \quad (4)$$

Using the decomposition of  $\bar{c}$ ,  $\bar{u}_j$  and  $\bar{S}$  as  $\bar{\varphi} = \langle \bar{\varphi} \rangle + \varphi''$ , applying the spatial-averaging method and according to the rules:  $\langle \varphi'' \rangle = 0$  and  $\langle \langle \bar{\varphi} \rangle \rangle = \langle \bar{\varphi} \rangle$ , Equation (4) can be expressed as:

$$\frac{\partial \langle \bar{c} \rangle}{\partial t} + \frac{\partial (\langle \bar{u}_j \rangle \langle \bar{c} \rangle)}{\partial x_j} + \frac{\partial (\langle \overline{u_j' c'} \rangle + \langle u_j'' c'' \rangle)}{\partial x_j} - \frac{\partial}{\partial x_j} \left( K_m \frac{\partial \langle \bar{c} \rangle}{\partial x_j} \right) + \langle \bar{S} \rangle = 0 \quad (5)$$

Equation (5) is the double-averaging advection-diffusion equation. The first term of the Equation (5) expresses the variation of the double-averaging SSC with time. The second term is the transport of advection flux resulted from the averaged flow velocity. The third term is the transport of diffusive flux related to the turbulent fluctuations  $u_j'$  and the fourth term is the transport of the dispersive flux associated with the spatial heterogeneity of time-averaging velocity field. The molecular diffusion term is ignored as it is much smaller than the turbulent diffusion and the dispersive flux. Assuming that no sediment is added into the river, therefore, the sediment source/sink term  $\langle \bar{S} \rangle$  can be written as  $-\partial(\omega \langle \bar{c} \rangle) / \partial x_3$  (i.e. the transport of sediment settling flux) in sandy flow, where  $\omega$  is the settling velocity of sediment particles.

Furthermore, in the steady uniform open channel flow, one has  $\frac{\partial \langle \bar{c} \rangle}{\partial t} = 0$ ,  $\partial(\langle \bar{u}_j \rangle \langle \bar{c} \rangle) / \partial x_j = 0$  for  $j=1, 2$  and  $3$ ,  $\partial(\langle \overline{u_j' c'} \rangle) / \partial x_j = 0$  and  $\partial(\langle u_j'' c'' \rangle) / \partial x_j = 0$  for  $j=1, 2$  (i.e. in both the longitudinal and the transverse directions). Equation (5) can then be simplified as:

$$\frac{\partial}{\partial x_3} (\langle \overline{u_3' c'} \rangle + \langle u_3'' c'' \rangle) - \frac{\partial(\omega \langle \bar{c} \rangle)}{\partial x_3} = 0 \quad (6)$$

The additional dispersive flux term needs to be appropriately determined in order to accurately simulate the vertical SSC profile in the steady equilibrium vegetated open channel sediment-laden flow.

## 2.2 The Dispersive Flux

The turbulent diffusion flux in Equation (6) is determined by the Fickian transport theory (van Rijn, 1984; Yang & Choi, 2010; Termini, 2019):

$$\langle \overline{u_3' c'} \rangle = -K_z \frac{\partial \langle \bar{c} \rangle}{\partial x_3} = -K_z \frac{\partial C}{\partial z} \quad (7)$$

where  $K_z$  represents the vertical turbulent diffusion coefficient. In Equation (7), for simplification,  $\langle \bar{c} \rangle$  is replaced by  $C$  to represent the time-spatial averaged SSC.

In flow without vegetation, the dispersive flux is usually ignored as it is much smaller than the turbulent flux. However, in the vegetated open channel flow, the dispersive flux cannot be ignored as the spatial heterogeneity is significantly strengthened by the presence of vegetation. This indicates that the dispersive flux has great effect on the vertical SSC profile in the vegetated open channel flow. In this study, we assume that the dispersive flux can be expressed as following:

$$\langle u_3 "c" \rangle = -K_D UC \quad (8)$$

where  $K_D$  is the dispersive coefficient,  $U$  is the longitudinal averaged velocity of cross-section and is used to scale the magnitude of the vertical averaged velocity that is difficult to obtain. Substituting Equations (7) and (8) into Equation (6) yields:

$$\frac{\partial}{\partial z} \left( -K_z \frac{\partial C}{\partial z} - K_D UC \right) - \frac{\partial(\omega C)}{\partial z} = 0 \quad (9)$$

The sediment advection-diffusion equation of fully developed steady flow can then be simplified as following:

$$\omega C + K_z \frac{dC}{dz} + K_D UC = A \quad (10)$$

where  $A$  is an integral constant. Equation (10) shows that the first term (the downward sediment settling flux) has to balance with the second and third terms (the upward diffusion and the dispersive fluxes). As no sediment is added into or jumps out of river at the water surface, the integral constant  $A$  is equal to zero. The Equation (10) then becomes:

$$\omega C + K_z \frac{dC}{dz} + K_D UC = 0 \quad (11)$$

The vertical SSC profile in the steady vegetated open channel flows can then be obtained by solving Equation (11).

In this study, the dispersive coefficient  $K_D$  that is related to the spatial heterogeneity in the vegetated open channel flow is defined as a function of the vertical coordinate  $z$ . In order to simplify the dispersive model, we assume that the dispersive coefficient is equal to the product of a scale factor  $K_f$  multiplying the morphological coefficient  $k_m$ :

$$K_D = K_f k_m \quad (12)$$

where the morphological coefficient  $k_m$  is a parameter reflecting the impact of flow field and vegetation (including the vegetation density, structure and arrangement) on dispersion; the scale factor  $K_f=0.001$  is used to eliminate the influence induced by the application of the longitudinal sediment flux  $UC$  rather than the vertical sediment flux  $u_3 C$  as well as to express the magnitude of the dispersive coefficient. Simulation shows that it is appropriate for the conditions investigated in this proposed model. According to the variation rules of the dispersive coefficient,  $k_m$  is equal to zero in the flow without vegetation, where the magnitude of the dispersion term is much smaller than the diffusion and advection terms.



The effect of dispersion is significant due to strong heterogeneity generated by the presence of vegetation. As discussed above, extensive experimental studies have been conducted to investigate the profile of the dispersive stress in the vegetated open channel flow. These studies (Poggi et al., 2004a; Rightetti, 2008; Stoesser & Nikora, 2008) showed that the variation of the dispersive stress was complicated but followed the similar law. They (Poggi et al., 2004a; Rightetti, 2008; Stoesser & Nikora, 2008) found that the dispersive stress increased from the zero at the channel bottom and reached the maximum value at almost the half height of vegetation and then decreased and approached zero at the top of vegetation. As such, the morphological coefficient can be parameterized as following:

$$k_m = \begin{cases} 0 & z \geq h & (a) \\ -\frac{2\theta}{h}z + 2\theta & \frac{h}{2} \leq z < h & (b) \\ \frac{2\theta}{h}z & z < \frac{h}{2} & (c) \end{cases} \quad (13)$$

where  $h$  is the height of vegetation and the parameter  $\theta$  is the value of the morphological coefficient at the half height of vegetation, where coefficient  $k_m$  reaches the maximum value. Equations (12) and (13) show that the dispersive coefficient is known when the value of  $\theta$  is determined. The maximum value of the morphological coefficient can be obtained by fitting the available experimental data of SSC for various vegetation conditions.

### 3 Method

In order to investigate the effect of the dispersive flux on the vertical SSC profile in the vegetated open channel flow, the turbulent diffusion flux and the sediment settling flux need to be determined. Nepf et al. (2004) conducted experiments to investigate the characteristic of the turbulent diffusion using the rigid straight rods as vegetation. The results showed that the turbulent diffusion coefficient approximated to the linear profile within the region of vegetation in the submerged vegetated open channel flow. The turbulent diffusion coefficient reached the maximum value at the top of vegetation and decreased linearly toward the water surface. Several formulas were proposed to simulate the turbulent diffusion coefficient in channels with the submerged vegetation. However, the turbulent diffusion coefficient remains almost a constant in the emergent vegetated open channel flow (Nepf, 1999). The settling velocity of sediments is another important parameter and can be estimated using the formula proposed by Zhang and Xie (1989) (see also Tan et al., 2018), which is applicable for both the laminar and the turbulent flow:

$$\omega = \sqrt{\left(13.95 \frac{\nu}{d}\right)^2 + 1.09 \frac{\gamma_s - \gamma_f}{\gamma_f} g d} - 13.95 \frac{\nu}{d} \quad (14)$$

where  $\nu$  represents the kinematic viscosity of water,  $g$  is the acceleration of gravity,  $\gamma_s$  and  $\gamma_f$  represent the bulk density of sediment and water, respectively,  $d$  is the representative size of sediment particles and the median size of sediments is used in this study.

The analytical solution of the vertical SSC profile can be obtained by solving the Equation (11) with the turbulent diffusion coefficient, the sediment settling velocity, as well as the dispersive coefficient determined in different vegetated open channel flows. The following sections introduce the methods for channels with the emergent and the submerged vegetation, respectively.

### 3.1 Channels with the Emergent Vegetation

Previous studies showed that majority of the flow momentum is absorbed by the vegetation elements induced drag instead of the resistance generated by channel bed in the vegetated open channel flows (Wilson, 2007; Tanino & Nepf, 2008b). The vertical turbulent diffusion coefficient  $K_z(z)$  is homogenized due to the presence of the emergent aquatic vegetation (Nepf, 1999, 2004) and can be expressed as the following in dense vegetation flow ( $a_v h > 0.1$ ) with the emergent cylindrical stems of uniform diameter:

$$K_z = \alpha^3 \sqrt{C_D a_v D U D} \quad (15)$$

where  $D$  is the diameter of vegetation stem,  $C_D$  is the drag coefficient of vegetation,  $a_v$  is the frontal area density of vegetation (expressed as  $a_v = nD$ ,  $n$  is the number of vegetation per unit area of channel bed) and  $\alpha$  is a proportional factor, which is taken as 0.2 for the vertical turbulent diffusion coefficient and as 0.8 for the lateral turbulent diffusion coefficient in the emergent vegetated open channel flow (Nepf, 2004). In addition,  $\alpha$  should slightly increase for the condition of dense vegetation. The value of  $C_D$  significantly depends on the density of vegetation and flow Reynolds number (Sonnenwald et al., 2019). In present study, according to the balance of vegetation drag with the streamwise component of gravity, the drag coefficient is evaluated as  $C_D = 2gs/(a_v U^2)$  (where  $s$  is the slope of channel bed) for experimental conditions of different vegetation densities (Huai et al., 2009b).

As the dispersive coefficient is different in the regions of  $z > h/2$  and  $z < h/2$ , the analytical solution of Equation (11) should be solved respectively at different layers with  $z = h/2$  as the critical height. Integrating Equation (11) using the turbulent diffusion coefficient determined by Equation (15) and the dispersive coefficient determined by Equations (12) and (13) yields the profiles of the vertical SSC in the emergent vegetated open channel flow:

$$C = C_a \exp\left(\frac{\theta K_f U}{h K_z} (z^2 - z_a^2) - \frac{2\theta K_f U + \omega}{K_z} (z - z_a)\right) \quad \text{for } z \geq \frac{h}{2} \quad (16a)$$

$$C = C_a \exp\left(-\frac{\theta K_f U}{h K_z} \left(z^2 - \frac{h^2}{4}\right) - \frac{\omega}{K_z} \left(z - \frac{h}{2}\right)\right) \quad \text{for } z < \frac{h}{2} \quad (16b)$$

where  $z_a$  and  $C_a$  are the referenced height and the corresponding referenced SSC, respectively. In this study,  $z_a$  is taken as the half height of the flow depth, namely  $z_a = H/2$  ( $H$  is the flow depth) and  $H = h$  in the emergent vegetated flow.

Experiments conducted by Lu (2008) and Ikeda et al. (1991) are used to fit the dispersive coefficient and to validate the analytical model. The experimental parameters are summarized in Table 1. In their experiments, SSC was measured in the emergent vegetated (rigid cylindrical

rods) flow for various vegetation densities. To calculate the vertical SSC profile, the turbulent diffusion coefficient  $K_z$  is calculated by using Equation (15) for experiments of Lu (2008). For comparing with the experiment of Ikeda et al. (1991) whose experimental vegetation density is beyond the applicable scope of Equation (15),  $K_z$  is, therefore, obtained as  $K_z = 0.09u_*h$  (where  $u_*$  is the friction velocity of flow), as suggested by Ikeda et al. (1991).

**Table 1.** Experimental parameters of Lu (2008) and Ikeda et al. (1991) in the emergent vegetated open channel flows.

Sources	Run number	$h(H)$ (m)	$D$ (m)	$s$ ( $10^{-3}$ )	$U$ (m/s)	$u_*$ (m/s)	$d$ (mm)	$a_v$ ( $m^{-1}$ )	$C_D$ /
Lu	D12-1	0.12	0.006	13.6	0.3343	0.1265	0.217	2.4	0.99
	D12-2	0.12	0.006	13.6	0.2918	0.1265	0.217	3.0	1.04
	D12-3	0.12	0.006	13.6	0.1690	0.1265	0.217	6.0	1.56
	D15-1	0.15	0.006	13.6	0.3321	0.1414	0.217	2.4	1.01
	D15-2	0.15	0.006	13.6	0.2932	0.1414	0.217	3.0	1.03
	D15-3	0.15	0.006	13.6	0.1700	0.1414	0.217	6.0	1.54
	D18-1	0.18	0.006	13.6	0.3436	0.1549	0.217	2.4	0.94
	D18-2	0.18	0.006	13.6	0.2947	0.1549	0.217	3.0	1.02
	D18-3	0.18	0.006	13.6	0.1692	0.1549	0.217	6.0	1.55
Ikeda	Run 9	0.05	0.005	6.67	0.2858	0.0572	0.145	1.0	1.60

### 3.2 Channels with the Submerged Vegetation

Flow structure, the turbulent diffusion and the dispersion in the submerged vegetated flow are much complicated than that in the emergent vegetated flow (Huai et al., 2009b; Nepf, 2012). As the expression of the dispersive and diffusion coefficients changes with water depth, Equation (11) needs to be solved at three layers to obtain the solution of SSC.

**Table 2.** Flow and sediment characteristics of experiments of Lu (2008) and Yuuki and Okabe (2002) in the submerged vegetated flow ( $k$  is the von Karman's constant).

Sources	Run number	$H$ (cm)	$h$ (cm)	$D$ (cm)	$d$ (mm)	$s$ ( $10^{-3}$ )	$u_*$ (cm/s)	$U$ (cm/s)	$k$ /	$a_v$ ( $m^{-1}$ )
Lu	C12	12	6.0	0.6	0.217	4.65	4.76	27.86	0.25	3
	C15	15	6.0	0.6	0.217	3.50	4.77	29.34	0.27	3
	C18	18	6.0	0.6	0.217	2.69	5.20	32.12	0.28	3
Yuuki and Okabe	Y1	6	3.5	0.2	0.100	1.00	2.13	22.70	0.20	2.08
	Y2	6	3.5	0.2	0.100	1.50	2.60	28.10	0.20	2.08
	Y3	6	3.5	0.2	0.100	2.00	3.01	31.90	0.20	2.08

Lu (2008) and Yuuki and Okabe (2002) conducted experiments to study the interaction of the suspended sediment load and vegetation in the submerged vegetated flow. These experiments are used for comparing and validating the present analytical model. Table 2 lists the parameters

and measurements of these two experiments. As the construction of experimental vegetation in these two experiments differs greatly from each other, the equations of the turbulent diffusion coefficient are also different, as demonstrated below.

Figure 2 is the sketch of the vertical turbulent diffusion coefficient and the morphological coefficient of the experiments of Lu (2008), in which the vegetation was modeled by rigid straight rods. Based on the study of Nepf (2012), the maximum value of the turbulent diffusion coefficient appears at the top of vegetation for flow with dense vegetation ( $a_v h > 0.1$ ) and can be expressed as:

$$K_z(z = h) = 0.032\Delta u h \quad (17)$$

where  $\Delta u$  represents the velocity difference between the wake region of vegetation and overflow, which is approximately equal to  $0.8u_H - u_w$  (where  $u_H$  is the flow velocity at the water surface and can be expressed as the logarithmical profile (Huai et al., 2019) and  $u_w = \sqrt{2gs / (C_D a_v)}$  is the averaged velocity in the wake region of vegetation and can be obtained according to the balance of gravity and drag (Huai et al., 2009b)). The diffusion coefficient is usually zero at the channel bed. In addition, in order to avoid the obvious mistake that the SSC is zero at the water surface caused by the approximation of  $K_z(z=H)=0$ , e.g. the solution of the classical Rouse equation (Rouse, 1937), the turbulent diffusion coefficient at the water surface of flow cannot be zero. The study of Elder (1959) showed that the depth-averaging turbulent diffusion coefficient is equal to  $ku_*H/6$ . In this study, the von Karman's constant (see Table 2) is smaller than 0.4, which is the value in clear water flow. For three conditions of Lu (2008), the mean value of the von Karman's constant  $k$  approximates to 0.26. Therefore, the expression of  $K_z$  is approximated as  $K_z(z = H) \approx 0.04u_*H$  at the water surface. The results show that the SSC modeled by this expression is consistent with the experimental observations near the water surface. After obtaining the values of  $K_z$  at three locations, namely the water surface, the top of vegetation and the channel bed, assuming a linear transition within the region of vegetation and overflow yields the expression of the vertical turbulent diffusion coefficient:

$$K_z = \begin{cases} k_2 z + b_2 & z \geq h \\ k_1 z + b_1 & z < h \end{cases} \quad (18)$$

where the parameters  $k_1$ ,  $k_2$ ,  $b_1$  and  $b_2$  differ in different experimental conditions. For experiments of Lu (2008), the parameters are calculated as  $k_1 = 0.032\Delta u$ ,  $b_1 = 0$ ,  $k_2 = (0.04u_*H - 0.032\Delta u h) / (H - h)$  and  $b_2 = 0.032\Delta u h - k_2 h$ . The dispersive coefficient in the vegetation region is simulated by using Equation (13) and is ignored in the overflow where the dispersive term is much smaller than the turbulent diffusion term.

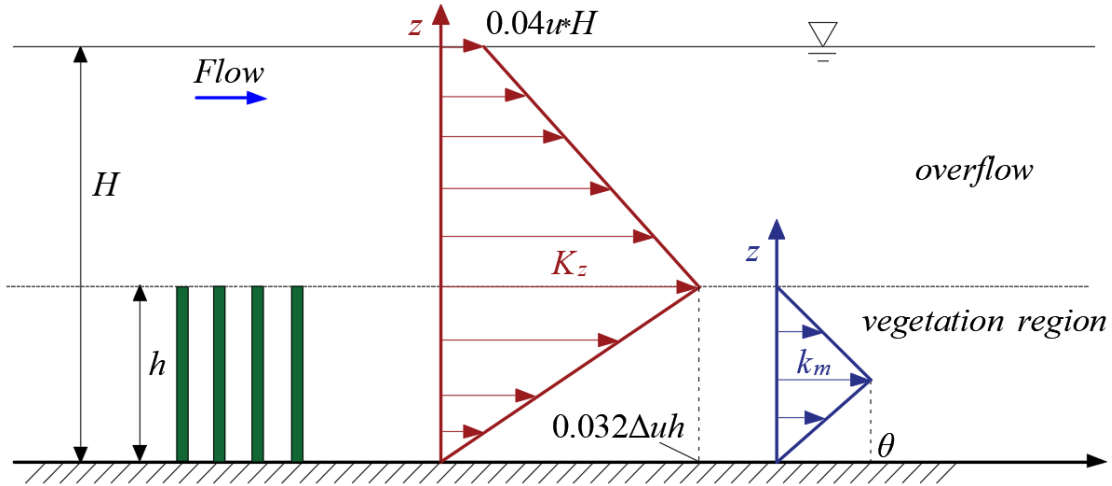


**Figure 2.** Sketch of the submerged vegetation and the profile of  $K_z$  and  $k_m$  in the experiment of Lu (2008).

Yuuki and Okabe (2002) carried out experiments in which the vegetation was composed of stagger-arrangement three-layer cylinders with averaged diameter  $D=2\text{mm}$ , as shown in Figure 3. The five branches significantly affect the value of the turbulent diffusion and the dispersive coefficient. Therefore, Equation (17) is not applicable for this experimental condition as it was established based on the experiments with the vegetation of straight rigid rods. However, the turbulent diffusion coefficient can still be divided into two layers according to the height of vegetation and is assumed to be linear profile in each layer (see Figure 3). According to the study of Yang and Choi (2010), the diffusion coefficient at the top of vegetation is  $K_z(z=h) = ku_*h$ , and  $K_z(z=0) = 0.1ku_*h$  is used at the bottom of channel where the turbulent diffusion coefficient is not zero according to the experimental observation in Yuuki and Okabe (2002). The four parameters are then calculated as  $k_2 = \frac{ku_*h}{h-H}$ ,  $b_2 = -\frac{ku_*hH}{h-H}$ ,  $k_1 = 0.8ku_*$  and  $b_1 = 0.1ku_*h$ , respectively. The referenced level  $z_a = H/2$  is also used for open channel flows with the submerged vegetation.

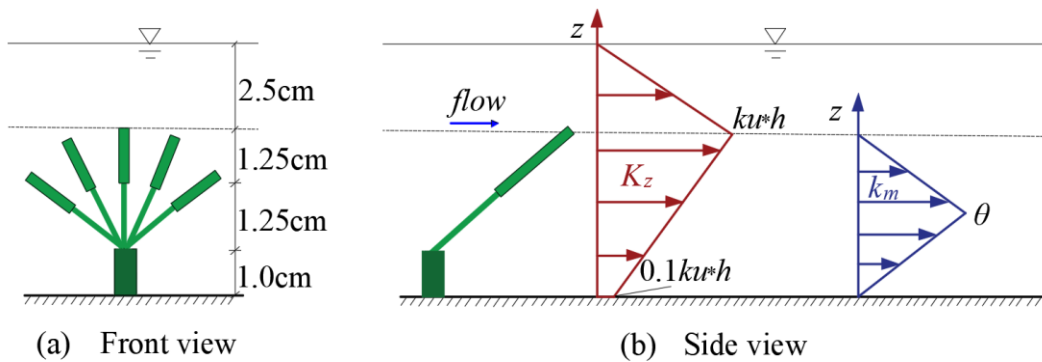


**Figure 3.** The sketch of the vegetation structure,  $K_z$  and  $k_m$  in the experiment of Yuuki and Okabe (2002). (a) The front view of the vegetation; (b) The side view of the vegetation, profile of the turbulent diffusion coefficient and the morphological coefficient.

The analytical solution of Equation (11) associated with various  $K_z(z)$  and  $k_m$  can then be obtained in three layers with some differences for these two experiments of different conditions, as described below.

For experiments of Lu (2008), the referenced height is in the overflow region, i.e.  $z_a \geq h$ . In the overflow region ( $z \geq h$ ), the effect of the vegetation induced dispersion is assumed to be small and can be ignored. Substituting Equations (18) and (13a) into (11), solving the ordinary differential equation obtains the SSC in the overflow region in the uniform submerged vegetated flow:

$$C(z) = C(z_a) \left( \frac{k_2 z + b_2}{k_2 z_a + b_2} \right)^{-\frac{\omega}{k_2}} \quad (19)$$

In the upper vegetation region, i.e.  $h/2 \leq z < h$ , the analytical solution of Equation (11) with consideration of the dispersion term is:

$$C(z) = C(h) \exp \left( \frac{r_1}{k_1} (z - h) \right) \left( \frac{k_1 z + b_1}{k_1 h + b_1} \right)^{\frac{\lambda_1 k_1 - r_1 b_1}{k_1^2}} \quad (20)$$

where  $r_1 = 2\theta K_f U / h$ ,  $\lambda_1 = -2\theta K_f U - \omega$  and  $C(h)$  denotes the SSC at the top of vegetation and can be calculated by Equation (19) as following:

$$C(h) = C_a \left( \frac{k_2 h + b_2}{k_2 z_a + b_2} \right)^{-\frac{\omega}{k_2}} \quad (21)$$

The analytical solution of SSC in the lower vegetation region (i.e.  $z < h/2$ ) is:

$$C(z) = C\left(\frac{h}{2}\right) \exp \left( \frac{r_2}{k_1} \left( z - \frac{h}{2} \right) \right) \left( \frac{k_1 z + b_1}{k_1 \frac{h}{2} + b_1} \right)^{\frac{\lambda_2 k_1 - r_2 b_1}{k_1^2}} \quad (22)$$

where  $r_2 = -2\theta K_f U / h$ ,  $\lambda_2 = -\omega$  and  $C(h/2)$  represents the SSC at the half height of vegetation and can be calculated by Equation (20).

In the experiments of Yuuki and Okabe (2002), the referenced height is within the vegetation region, i.e.  $h/2 < z_a = H/2 < h$ . Therefore, the analytical solution of the profile of SSC differs from above. In the upper vegetation region, i.e.  $h/2 \leq z \leq h$ , the analytical solution of Equation (11) with consideration of the dispersion term is:

$$C(z) = C(z_a) \exp\left(\frac{r_1}{k_1}(z - z_a)\right) \left(\frac{k_1 z + b_1}{k_1 z_a + b_1}\right)^{\frac{\lambda_1 k_1 - r_1 b_1}{k_1^2}} \quad (23)$$

In the overflow region ( $z > h$ ), the effect of vegetation induced dispersion is assumed to be small and can be ignored. Substituting Equations (18) and (13a) into (11) and solving the (11) yields SSC:

$$C(z) = C(h) \left(\frac{k_2 z + b_2}{k_2 h + b_2}\right)^{-\frac{\omega}{k_2}} \quad (24)$$

where  $C(h)$  can be calculated by the Equation (23).

The analytical solution of SSC in the lower vegetation region (i.e.  $z < h/2$ ) is:

$$C(z) = C\left(\frac{h}{2}\right) \exp\left(\frac{r_2}{k_1}\left(z - \frac{h}{2}\right)\right) \left(\frac{k_1 z + b_1}{k_1 \frac{h}{2} + b_1}\right)^{\frac{\lambda_2 k_1 - r_2 b_1}{k_1^2}} \quad (25)$$

where  $C(h/2)$  represents the SSC at the half height of vegetation and can be calculated by Equation (23).

## 4 Results

### 4.1 Emergent Vegetation

Figures 4 and 5 show the comparison of the predicted and measured vertical profiles of SSC for experiments of Ikeda et al. (1991) and Lu (2008), respectively. It is seen that the analytical solution ignoring the dispersive term, i.e.  $\theta=0$  (blue dashed lines in Figures 4 and 5), greatly under-predicts SSC above the half height of flow depth and significantly over-predicts SSC within half height of flow depth. This indicates that the effect of the dispersive flux on the vertical SSC distribution in the vegetated open channel flows is significant and cannot be ignored in calculating the vertical SSC profile. It is seen from Figures 4 and 5 that the dispersive coefficient is usually negative, which means that the direction of the dispersive flux is opposite to the settling flux. According to the mass conservation, the total upward flux, i.e. the sum of the diffusion flux and the dispersive flux, has to balance with the settling flux. Therefore, the opposite dispersive flux weakens the effect of the settling flux on the total vertical SSC profile. In addition, the SSC decreases in the region near the river bed and increases in the region near the water surface with the increase of the absolute value of the dispersive coefficient. However, when the absolute value of the dispersive coefficient is very large, the deviation between the predicted and measured SSC becomes larger again, while the sediment concentration changes from over-predicted to under-predicted within the half height of the flow depth.

In Figure 5, values of  $H$  and  $a_v$  for different experiments are showed in the figure for convenience of comparison. Results with the same vegetation density but different flow depths (i.e. Figures 5(a), (d) and (g); Figures 5(b), (e) and (h); and Figures 5(c), (f) and (i)) show that the

relationship between the dispersive coefficient and flow depth is not very clear. However, the comparison of the same flow depth but different vegetation densities, i.e. Figures 5(a-c), (d-f) and (g-i), shows that the vegetation density has significant impact on the dispersive coefficient. Specifically, the maximum absolute values of the averaged fitting morphological coefficient are -10, -3.7, -3.5 and -4, corresponding respectively to the vegetation density of 1, 2.4, 3 and  $6\text{m}^{-1}$ . In general, Figure 5 demonstrates that the absolute value of the morphological coefficient decreases with the increase of the vegetation density with the exception of the case  $a_v = 6\text{m}^{-1}$ . This exception case may be ascribed to the following fact: in the experiment of Lu (2008), the arrangement of the vegetation was regular and in the cases of D12/D15/D18-3, i.e.  $a_v = 6\text{m}^{-1}$ ; the transverse and longitudinal interval between the vegetation centers was respectively 2cm and 5cm. For this exception case, i.e.  $a_v = 6\text{m}^{-1}$ , the ratio of the transverse interval over the longitudinal interval was 0.4, while this ratio was approximate to one in the cases of  $a_v = 1, 2.4$  and  $3\text{m}^{-1}$ . However, the conclusions of the dispersive rules and empirical coefficient  $\alpha$  of Equation (15) are obtained from the experiments of stagger arrangement where the ratio of the transverse interval over the longitudinal interval is approximate to one. From this aspect, the unusual result for condition  $a_v = 6\text{m}^{-1}$  may be caused by the arrangement of vegetation, which requires further experimental study for confirmation.

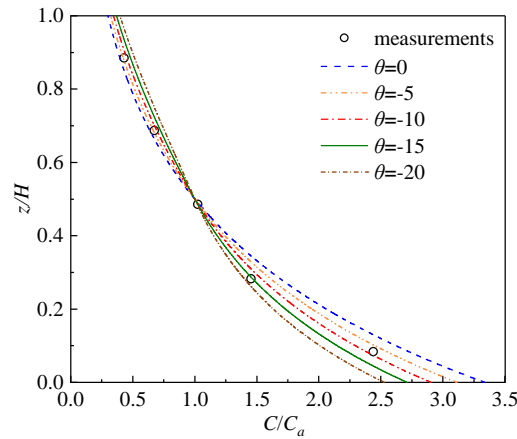


**Figure 4.** Comparison of the vertical SSC profiles of the predicted (lines for different morphological conditions) by Equations (16a, b) and measured (open circles, Ikeda et al., 1991).



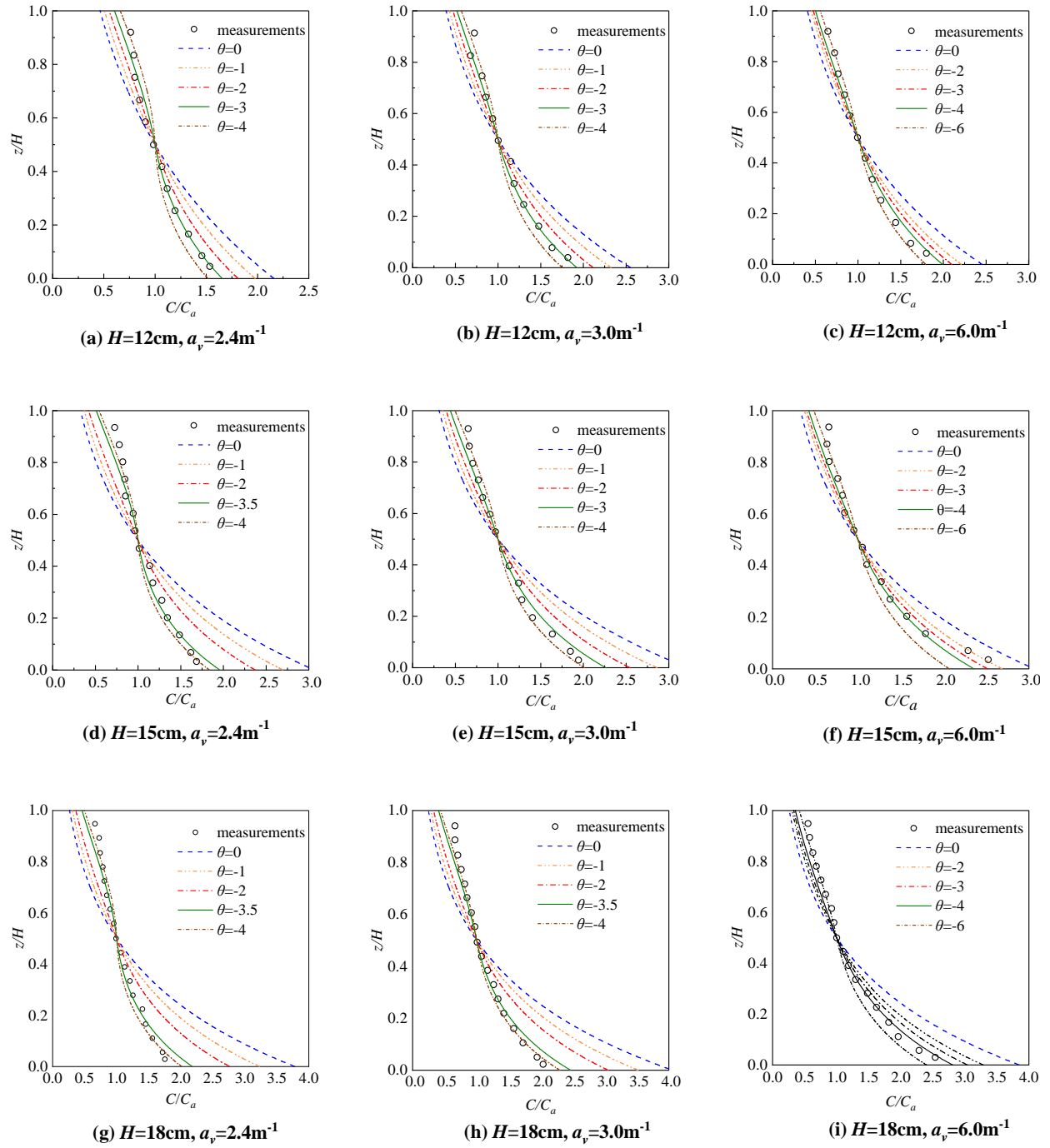


**Figure 5.** Comparison of the vertical SSC profiles of the predicted (lines for different morphological conditions) by Equations (16a, b) and experimentally measured (open circles, Lu, 2008) for different vegetation heights and densities. As shown in figure: (a) D12-1; (b) D12-2; (c) D12-3; (d) D15-1; (e) D15-2; (f) D15-3; (g) D18-1; (h) D18-2; (i) D18-3.

## 4.2 Submerged Vegetation

Figure 6 shows the comparison of the predicted and measured vertical SSC profiles in the submerged vegetated open channel flows. In the experiments of Lu (2008), the ratio of the flow depth over the vegetation height varies while the vegetation density is fixed (see Table 2 for details of the flow conditions). Figures 6(a)(b)(c) show that the deviation of the predicted SSC from the measured SSC decreases with the increase of the vegetation submergence for the condition without the dispersive term (i.e. blue dashed lines). This indicates that the effect of the vegetation on the vertical SSC profile is weakened with the increase of the vegetation submergence (i.e.  $H/h$  increases). This may be because the relative importance of the vegetation drag over the bed friction drag decreases for high vegetation submergence (Raupach et al., 1996; Nepf & Vivoni, 2000; Nepf, 2012). Figures 6(a)(b)(c) show that  $\theta=-3$  (i.e. green solid lines) better represents the vegetation induced dispersive coefficient, indicating that the dispersive coefficient has little relationship with the vegetation submergence for the flow conditions of Lu (2008).

The values of the dispersive coefficient for the experiments of Yuuki and Okabe (2002) are slightly larger than the values in the experiments of Lu (2008). This may be ascribed to the fact that the vegetation structure in the experiments of Yuuki and Okabe (2002) favors the dispersion. It is seen from Figure 6(d) that the vertical SSC profile can be reasonably predicted with the dispersive coefficient  $\theta=-3$ , while Figures 6(e)(f) show that some deviations exist between the predicted and the measured SSC. This may be due to the complicated vegetation structure in their experiments, indicating that the analytical model proposed in this study has some defects and cannot provide accurate prediction of the SSC in such complicated vegetation structure. Nevertheless, the predicted SSC for the experiments of Yuuki and Okabe (2002) is much better than the previous similar study (see Figure 10 in Yang and Choi (2010)), which did not consider the effect of the dispersive term.

Analysis of the results shows that the analytical solution agrees well with experimental measurements in the region of overflow. For regular arrangement of straight cylinders (i.e. the experiments of Lu (2008)),  $a_v=3\text{m}^{-1}$ , the vertical SSC profile within the vegetation region can be accurately predicted using the analytical approach proposed in this study with an appropriate dispersive coefficient. For the staggered vegetation with complicated structure (i.e. the experiments of Yuuki and Okabe (2002)),  $a_v=2.08\text{m}^{-1}$ , some deviation between the analytical prediction and the measurement exists within the vegetation region. The variation of the vertical SSC profile with the dispersive coefficient found in the emergent vegetated flow also appears in the submerged vegetated flow, i.e. the SSC decreases with the increase of the absolute value of the dispersive coefficient in the vegetated region.

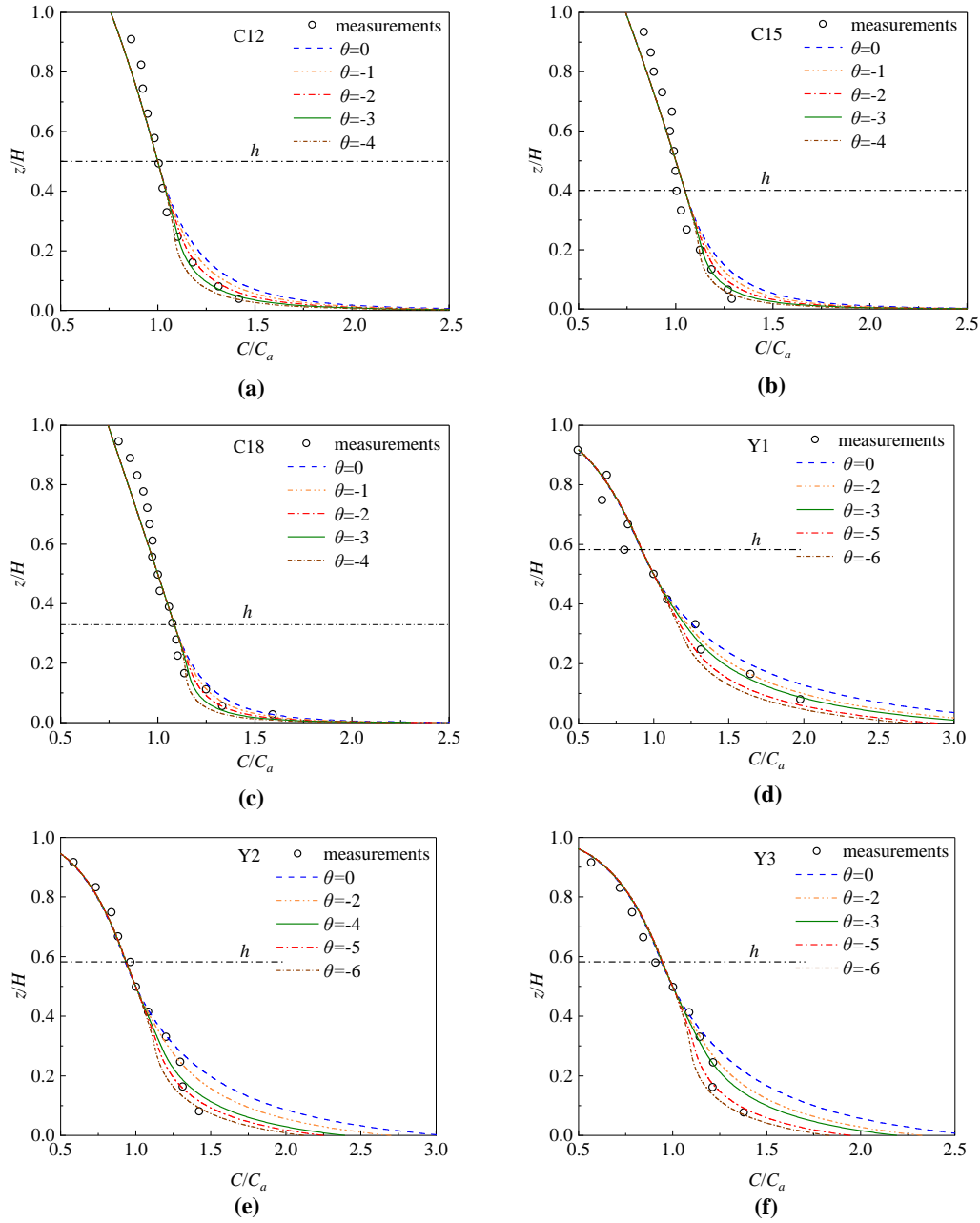


**Figure 6.** The comparison between analytically predicted (lines) and experimentally measured (Lu (2008) and Yuuki and Okabe (2002): open circles) vertical SSC profile in the submerged vegetated flow.

### 4.3 Analysis

Result of Figures 4, 5 and 6 shows that the analytical solutions either over-predict or under-predict the SSC at different regions of the vegetated open channel sediment-laden flow. In

order to represent the deviation of the predicted SSC from the observed SSC for different values of  $\theta$ , the averaged error ( $AE$ ) is defined as following:

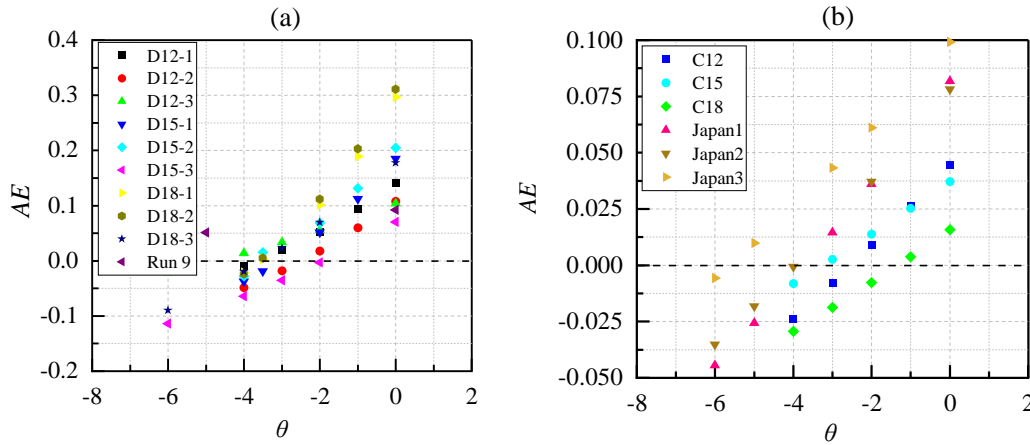
$$AE = \frac{\sum (C_{pre} - C_{obs})}{N} \quad (26)$$

where  $N$  is the sampling number of the observed SSC in the vertical direction at a monitoring position in the experiments,  $C_{obs}$  is the observed SSC and  $C_{pre}$  represents the predicted SSC by the proposed model.

In order to determine the best-fitted value of  $\theta$ , another common statistical parameter, i.e. the mean relative error ( $MRE$ ), is also used to evaluate the error of the proposed model:

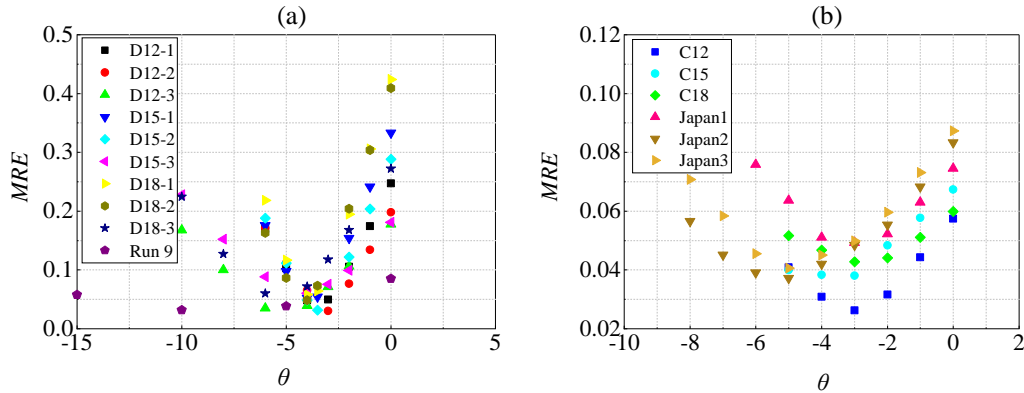
$$MRE = \frac{\sum \frac{|C_{pre} - C_{obs}|}{C_{obs}}}{N} \quad (27)$$

Figure 7 shows the relationship between the  $AE$  and  $\theta$  for both the emergent and the submerged vegetated open channel flow, which clearly demonstrates whether the model over-predicts or under-predicts SSC. It is seen from Figure 7 that the SSC is usually over-predicted by the proposed model (the positive value of  $AE$ ) for the  $\theta=0$ . With the increase of the absolute value of  $\theta$ , the SSC simulated by the proposed model varies from the over-predicted to the under-predicted (the negative value of  $AE$ ) for both the submerged and the emergent vegetated open channel flow. The scope of  $\theta$  corresponding to  $AE=0$  in the emergent vegetated open channel flow is much more centralized than that in the channel with the submerged vegetation. The specific best-fitted value of  $\theta$  can be determined by the variation of  $MRE$  calculated by Equation (27).



**Figure 7.** The variation of the vertical averaged error between the predicted and observed SSC with  $\theta$ . (a) the emergent vegetated open channel flow; (b) the submerged vegetated open channel flow.

Figure 8 is the variation of  $MRE$  with  $\theta$  for open channel flow with both the emergent (Figure 8(a)) and the submerged (Figure 8(b)) vegetation, respectively. Figure 8 shows that  $MRE$  decreases firstly and then increases with the increase of  $\theta$ . The value of  $\theta$  corresponding to the smallest  $MRE$  is known as the best-fitted value for that condition, which is listed in the last column of Table 3. Small  $MRE$  indicates that the model proposed in this study can accurately simulate the vertical profile of SSC in the vegetated open channel flow. The suggested value of  $\theta$  is from -5 to -3 for the channels with the range of vegetation density  $a_v$  being from 2 to  $6\text{m}^{-1}$ . More specifically, the best-fitted value of  $\theta$  approximates to -4 with the range of the vegetation density being from 2 to  $6\text{m}^{-1}$  in the open channel flow with the emergent vegetation. More experiments and studies are required to explore the rules of the dispersive coefficient in the open channel flow with the vegetation density outside the scope of  $2\text{m}^{-1} < a_v < 6\text{m}^{-1}$ .



**Figure 8.** The variation of the  $MRE$  with  $\theta$ : (a) the emergent vegetated open channel flow; (b) the submerged vegetated open channel flow.

**Table 3.** The parameters and the best-fitted value of  $\theta$  for open channel flow with the emergent and the submerged vegetation.

Conditions	Run number	$Re_s$	$a_v(\text{m}^{-1})$	$\theta$
Emergent vegetation	D12-1	1994	2.4	-3
	D12-2	1740	3	-3
	D12-3	1008	6	-4
	D15-1	1981	2.4	-4
	D15-2	1749	3	-3.5
	D15-3	1014	6	-4
	D18-1	2049	2.4	-4
	D18-2	1758	3	-4
	D18-3	1009	6	-4
Submerged vegetation	Run 9	1420	1	-10
	C12	991	3	-3
	C15	859	3	-3
	C18	753	3	-3
	Y1	153	2.08	-3
	Y2	187	2.08	-4
	Y3	217	2.08	-5

Above discussion shows that the magnitude of the dispersive coefficient is mainly influenced by the flow field (mainly velocity) and the vegetation characteristics (density, structure). The flow field can be represented by using the stem Reynolds number, i.e.  $Re_s = \frac{u_w D}{\nu}$ . The complicated vegetation structure enhances the dispersive strength through influencing the flow turbulence and the spatial heterogeneity, which can be proved by comparing the values of  $\theta$  between the experiments of Yuuki and Okabe (2002) and the experiments of Lu (2008). Table 3 lists the stem Reynolds number, the vegetation density and the best-fitted  $\theta$ . The vegetation density for the experiments of Yuuki and Okabe (2002) (i.e. conditions Y1, Y2 and Y3) is all 2.08, while the stem Reynolds number increases gradually. Therefore, the results of Y1, Y2 and Y3 indicate that the dispersion increases with the increase of  $Re_s$ , which may be caused by the strong turbulence induced by the large stem Reynolds number and corresponding intensive spatial heterogeneity. The value of  $\theta$  for the experiments C12, C15 and C18 is all -3, while the stem Reynolds number varies slightly. This phenomenon may be ascribed to the fact that the vegetation structure of C12, C15 and C18 is regular and variation of the stem Reynolds number is small.

For both the emergent and the submerged vegetated open channel flow investigated in this study, Figure 9 shows that the averaged absolute value of  $\theta$  decreases with the increase of the vegetation density, where  $\theta$  is obtained by averaging the value of  $\theta$  for the conditions of the same vegetation density. The results show that the gradient of the morphological coefficient with the vegetation density is large for the condition  $a_v < 2.08 \text{ m}^{-1}$ , while the gradient is small for dense vegetation conditions investigated in this study. Within the vegetation region, the stem wakes become a localized source of turbulence such that the turbulent flow field is much more heterogeneous than that in the region without vegetation (Nepf et al., 1997). Thus, the dispersive coefficient is significantly increased by the presence of vegetation for small vegetation density. The interval between the vegetation stem's centers decreases gradually with the increase of the vegetation density, leading to the decrease of characteristic area of spatial averaging. Therefore, the vegetation-induced vortices may overlap in the characteristic area, which weakens the local inhomogeneity, and thus the dispersive coefficient decreases. Figure 9 also shows that the dispersive coefficient increases again when the vegetation density increases to  $a_v = 6 \text{ m}^{-1}$ . This could be caused by the arrangement of vegetation for the case of  $a_v = 6 \text{ m}^{-1}$ . More experiments are needed for better understanding and interpretation of the phenomenon.

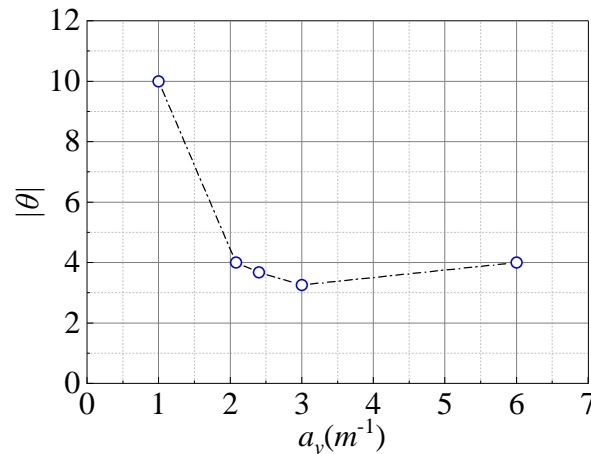


**Figure 9.** The variation of the absolute value of the maximum morphological (dispersive) coefficients with the vegetation density.

## 5 Discussion

The simulation of SSC in the vegetated open channel sediment-laden flow is very complicated. It requires well-defined flow field including flow velocity and turbulence strength, as well as the sediment particle characteristics. The empirical equations of the vertical turbulent diffusion coefficient used for conditions of Lu (2008) are obtained from the previous flume experiments (Nepf, 1999, 2004, 2012), which are interpreted as that the same straight rigid rods are used as the experimental vegetation and the vegetation density is within the scope of these formulas. For other conditions used in this study, experimental conditions are outside the scope of these formulas. As such, the turbulent diffusion coefficient has to be determined by the corresponding experimental observations or previous studies (Yang & Choi, 2010). The model proposed in this study is based on the correct determination of the turbulent diffusion coefficient model. Therefore, it is still a challenge task to extend the present model to open channel flow with the natural live (flexible) vegetation. Nevertheless, the proposed model is a simple and effective tool for simulating the vertical profile of SSC in the open channel flow with vegetations.

The double-averaging method, in which the classical time-averaging advection-diffusion equations are averaged over spatial area in the plane parallel to the bottom of channel, is used to simulate the vertical SSC profile in the vegetated open channel flow. The application of the double-averaging method for flow field analysis reduces the discordance resulted from the spatial heterogeneity within the vegetation region. In order to solve the double-averaging advection-diffusion equations, the diffusive flux is expressed by the Fickian diffusion model, while the dispersive flux is the product of the dispersive coefficient  $K_D$  and the mass flux  $CU$ . According to the previous experiments and the results of this study, the proposed dispersive model generalizes the influences of the dispersion as the function of coordinate  $z$ . As such, the size of the spatial averaging is not emphasized in this study. The suggestion about the size of the spatial averaging is that it must represent the spatial heterogeneity to reduce the error induced by the variation of the spatial averaging size. For example, it is correct to use the whole domain parallel to the bed as the size of the spatial averaging for open channel flow with irregular staggered vegetation or rough bed (Nikora et al., 2007b). For open channel flow with regular staggered vegetation, the region of the adjacent four vegetations is suggested as the size of the spatial averaging (Yuuki & Okabe, 2002; Poggi et al., 2004b).

There is little knowledge about the dispersive coefficient model, while most previous investigations focused on the dispersive stress obtained from the experimental measurements. Experiments with natural vegetation (*salix pentandra*) showed that the distribution of the dispersive stress is very complicated (Righetti, 2008) in which the magnitude of the dispersive stress at the top of vegetation and river bed is smaller than that at the half height of vegetation. Poggi and Katul (2008b) and Coceal et al. (2008) carried out experiments using rigid straight vegetation. Their results showed that the maximum value of the dispersive stress occurred at almost the half height of vegetation and decreased toward both up and down vertical directions. The results also showed that the magnitude of the dispersive stress greatly depended on the vegetation density. Based on these laboratory experimental studies, the authors assume that the

variation of the dispersive flux, i.e.  $\langle u_3 "c" \rangle = -K_D UC$ , in the vegetated open channel flow is similar to that of the dispersive stress. For simplification, the authors further assume that the dispersive coefficient  $K_D$  is a triangle profile in the vegetation region as expressed in Equations (12) and (13). The comparison of the SSC profile simulated by proposed model with the experimental measurements confirms the strong relation between dispersive coefficient and the vertical SSC profile in the vegetated open channel flows.

Results show that the dispersive term (usually appearing as negative value) plays an important role in determining the vertical SSC profile in the vegetated suspended sediment-laden flow. For the emergent vegetated flow, the model calculated SSC from the half height of the vegetation to the channel bottom varies from over-prediction to under-prediction with the increase of the absolute value of the dispersive coefficient, while the predicted SSC above the half height of vegetation has opposite variation trend (see Figures 4 and 5). For the submerged vegetated flow, the variation of SSC within the vegetation region is similar to that under the half height of vegetation of the emergent vegetated flow (see Figure 6). This means that the appropriate dispersive coefficient can be obtained by fitting the experimental data. Because all the dispersive coefficients are modeled as triangle profile, the maximum value of the morphologic coefficient (i.e.  $\theta$ ) is used to represent the magnitude of the dispersive coefficient. The relationship between the best-fitted value of  $\theta$  and the vegetation density, the vegetation structure and the stem Reynolds number depends on the experimental conditions. This means that the best-fitted values of  $\theta$  proposed in this paper can only represent the conditions investigated in this study. However, the rules between  $\theta$  and  $a_v$ ,  $Re_s$  and the vegetation structure conform to the physical mechanism and are strongly supported by previous relevant experimental studies.

## 6 Conclusions

In this paper, the model of the dispersive coefficient is proposed based on the concept of the dispersion to investigate the vertical SSC profile in the vegetated suspended sediment-laden flow. The double-averaging method is applied to simulate the vertical SSC profile in the vegetated open channel flow with time-spatial averaging advection-diffusion equations. The proposed model is validated by comparing the analytical solution of the vertical SSC profile with the existing experimental measurements. Results show that the proposed model of the dispersive coefficient is reliable and can be used to estimate the vertical SSC profile in the complicated vegetated, sediment-laden open channel flow. The following conclusions can be drawn from this study.

(1) A model for estimating the dispersive coefficient is proposed in this study based on the concept of the dispersion. For both the emergent and the submerged vegetated open channel flow investigated in this study, the dispersive coefficient decreases with the increase of the vertical axis  $z$  from the half height of the vegetation and increases with the increase of  $z$  from the channel bottom to the half height of vegetation. The dispersive coefficient reaches zero at both the top of the vegetation and the channel bottom.

(2) The effect of the dispersion on the vertical SSC profile within the vegetation region is significant and cannot be ignored. The inclusion of the dispersive term can greatly improve the prediction of the vertical SSC profile in the vegetated region and the region close to the channel



bottom. The dispersive term can be extended to the roughness bed or rivers with sand ripples, where the spatial heterogeneity of flow structure is also strong owing to the complicated uneven channel morphology.

(3) The double-averaging method is applied to simulate the vertical SSC profile in the vegetated open channel flow for improving the prediction of SSC. This is particularly important in the region of vegetation, where the spatial heterogeneity of the turbulent flow is strong owing to the presence of vegetation.

(4) The fitted morphological coefficient is mainly related to the vegetation density, the flow field and the vegetation structure in this study. For the conditions investigated in this study, the absolute values of the morphological and the dispersive coefficients decrease sharply with the increase of vegetation density, then increase slightly with the increase of vegetation density.

(5) The suggested range of  $\theta$  is -5 to -3 with the mean related error smaller than 10% when the vegetation density  $a_v$  is within the range from 2 to  $6\text{m}^{-1}$ . Owing to the limited available experimental data, it is not clear what is the variation trend of the dispersive coefficient for sparse vegetation density (i.e.  $a_v < 1\text{m}^{-1}$ ) and very dense vegetation density (i.e.  $a_v > 6\text{m}^{-1}$ ). Further experiments with a wide range of the vegetation density are required to accurately propose the dispersive model.

## Acknowledgments

All the data used in this work have been reported elsewhere (Ikeda et al., 1991; Yuuki & Okabe, 2002; Lu, 2008). The research reported here is financially supported by the Natural Science Foundation of China (Nos. 11872285 and 11672213), The UK Royal Society – International Exchanges Program (IES\R2\181122) and the Open Funding of State Key Laboratory of Water Resources and Hydropower Engineering Science (WRHES), Wuhan University (Project No: 2018HLG01). Comments made by Reviewers have greatly improved the quality of the final paper.

There are no real or perceived financial conflicts of interests for any author, no other affiliations for any author that may be perceived as having a conflict of interest with respect to the results of this paper.

## Nomenclature

$A$	integral constant
$a_v$	the frontal area density of vegetation
$b_1, b_2$	parameters of expression of turbulent diffusion coefficient profile at region $z < h$ and $z \geq h$ respectively in submerged vegetated open channel flows
$C$	time-spatial averaging suspended sediment concentration
$C_a$	referenced suspended sediment concentration at referenced height
$C_D$	drag coefficient of vegetation

$C_{pre}$	predicted suspended sediment concentration by this model
$C_{obs}$	observed suspended sediment concentration in experiments
$c$	instantaneous suspended sediment concentration
$D$	diameter of vegetation
$d$	representative size of sediment particles
$f, \varphi$	two different variables
$g$	acceleration of gravity
$H$	flow depth
$h$	height of vegetation
$K_D$	dispersive coefficient
$K_f$	a scale factor and $K_f=0.001$ in present study
$K_m$	molecular diffusion coefficient
$K_z$	vertical turbulent diffusion coefficient
$k$	von Karman's constant
$k_1, k_2$	gradients of expression of turbulent diffusion coefficient profile at region $z < h$ and $z \geq h$ respectively in submerged vegetated open channel flows
$k_m$	morphological coefficient
$N$	sampled number of the observed SSC in the vertical direction at a monitor point in the experiments
$n$	number of vegetation per unit area
$r_1, \lambda_1$	two parameters
$Re_s$	stem Reynolds number
$r_2, \lambda_2$	two parameters
$S$	source or sink of sediment in advection-diffusion equation
$s$	slope of channel bed
$t$	time
$U$	averaged longitudinal flow velocity of cross-section
$u$	instantaneous longitudinal flow velocity
$u_*$	friction velocity
$u_w$	averaged velocity in the wake region of vegetation
$u_H$	flow velocity at the water surface
$u_j$	instantaneous flow velocity component in $j$ th direction

$u_1, u_2, u_3$	instantaneous flow velocity of longitudinal, transverse and vertical, respectively
$x_j$	the $j$ th direction, $x_1=x$ , $x_2=y$ and $x_3=z$ are directions of longitudinal, transverse and vertical, respectively
$z$	vertical coordinate
$z_a$	referenced height
$\alpha$	a proportional factor
$\gamma_f$	the bulk density of water
$\gamma_s$	the bulk density of sediment
$\sigma$	a constant
$\nu$	the kinematic viscosity of water
$\omega$	settling velocity of sediment particles
$\theta$	values of morphological coefficient at the half height of vegetation
$\Delta u$	velocity difference between the region of vegetation wake and overflow
'	the deviation of instantaneous variables from time averaging variables
"	the deviations of time averaged variables from spatial averaged variables
-	time average
< >	spatial average
< - >	time-spatial average

699

## 700 References

- 701 Boudreault, L., Dupont, S., Bechmann, A., & Dellwik, E. (2017). How forest inhomogeneities  
702 affect the edge flow. *Boundary-Layer Meteorology*, 162(3), 375-400.  
703 <https://doi.org/10.1007/s10546-016-0202-5>
- 704 Coceal, O., Thomas, T. G., & Belcher, S. E. (2007). Spatial Variability of Flow Statistics within  
705 Regular Building Arrays. *Boundary-Layer Meteorology*, 125(3), 537-552.  
706 <https://doi.org/10.1007/s10546-007-9206-5>
- 707 Coceal, O., Thomas, T. G., & Belcher, S. E. (2008). Spatially-averaged flow statistics within a  
708 canopy of large bluff bodies: Results from direct numerical simulations. *Acta*  
709 *Geophysica*, 56(3), 862-875. <https://doi.org/10.2478/s11600-008-0025-y>
- 710 Coceal, O., Thomas, T. G., Castro, I. P., & Belcher, S. E. (2006). Mean Flow and Turbulence  
711 Statistics over Groups of Urban-like Cubical Obstacles. *Boundary-Layer Meteorology*,  
712 121(3), 491-519. <https://doi.org/10.1007/s10546-006-9076-2>
- 713 Elder, J. W. (1959). The dispersion of marked fluid in turbulent shear flow, *Journal of Fluid*  
714 *Mechanics*, 5(4), 544-560. <https://doi.org/10.1017/S0022112059000374>

- Florens, E., Eiff, O., & Moulin, F. (2013). Defining the roughness sublayer and its turbulence statistics. *Experiments in Fluids*, 54(4). <https://doi.org/10.1007/s00348-013-1500-z>
- Fu, X. D., Wang, G. Q., & Shao, X. (2005). Vertical dispersion of fine and coarse sediments in turbulent open-channel flows, *Journal of Hydraulic Engineering*, 10(131), 877-888. [https://doi.org/10.1061/\(ASCE\)0733-9429\(2005\)131:10\(877\)](https://doi.org/10.1061/(ASCE)0733-9429(2005)131:10(877))
- Han, X., He, G. J., & Fang, H. W. (2017). Double-averaging analysis of turbulent kinetic energy fluxes and budget based on large-eddy simulation. *Journal of Hydrodynamics*, 29(4), 567-574. [https://doi.org/10.1016/S1001-6058\(16\)60769-2](https://doi.org/10.1016/S1001-6058(16)60769-2)
- Huai, W. X., Chen, Z. B., Han, J., Zhang, L. X., & Zeng, Y. H. (2009b). Mathematical model for the flow with submerged and emerged rigid vegetation. *Journal of Hydrodynamics*, 21(5), 722-729. [https://doi.org/10.1016/S1001-6058\(08\)60205-X](https://doi.org/10.1016/S1001-6058(08)60205-X)
- Huai, W. X., Yang, L., Wang, W. J., Guo, Y. K., Wang, T., & Cheng, Y. G. (2019). Predicting the vertical low suspended sediment concentration in vegetated flow using a random displacement model. *Journal of Hydrology*, 578, 124101. <https://doi.org/10.1016/j.jhydrol.2019.124101>
- Huai, W. X., Zeng, Y. H., Xu, Z. G., & Yang, Z. H. (2009a). Three-layer model for vertical velocity distribution in open channel flow with submerged rigid vegetation. *Advances in Water Resources*, 32(4), 487-492. <https://doi.org/10.1016/j.advwatres.2008.11.014>
- Ikeda, S., Izumi, N., & Ito, R. (1991). Effects of pile dikes on flow retardation and sediment transport. *Journal of Hydraulic Engineering*, 11(117), 1459-1478. [https://doi.org/10.1061/\(ASCE\)0733-9429\(1991\)117:11\(1459\)](https://doi.org/10.1061/(ASCE)0733-9429(1991)117:11(1459))
- Kim, H. S., Kimura, I., & Park, M. (2018). Numerical simulation of flow and suspended sediment deposition within and around a circular patch of vegetation on a rigid bed. *Water Resources Research*, 54(10), 7231-7251. <https://doi.org/10.1029/2017WR021087>
- Kundu, S. (2019). Modeling stratified suspension concentration distribution in turbulent flow using fractional advection–diffusion equation, *Environmental Fluid Mechanics*, 19(6), 1557-1574. <https://doi.org/10.1007/s10652-019-09679-9>
- Le Bouteiller, C., & Venditti, J. G. (2015). Sediment transport and shear stress partitioning in a vegetated flow, *Water Resources Research*, 51(4), 2901-2922. <https://doi.org/10.1002/2014WR015825>
- Li, D., Yang, Z. H., Sun, Z., Huai, W. X., & Liu, J. (2018). Theoretical model of suspended sediment concentration in a flow with submerged vegetation. *Water*, 10(11), 1656. <https://doi.org/10.3390/w10111656>
- Li, S., & Katul, G. (2019). Cospectral budget model describes incipient sediment motion in turbulent flows. *Physical Review Fluids*, 4(9), 093801. <https://doi.org/10.1103/PhysRevFluids.4.093801>
- Li, S., Katul, G., & Huai, W. (2019). Mean velocity and shear stress distribution in floating treatment wetlands: An analytical study. *Water Resources Research*, 55(8), 6436-6449. <https://doi.org/10.1029/2019WR025131>
- Li, S., Shi, H., Xiong, Z., Huai, W., & Cheng, N. (2015). New formulation for the effective relative roughness height of open channel flows with submerged vegetation. *Advances in Water Resources*, 86, 46-57. <https://doi.org/10.1016/j.advwatres.2015.09.018>

- Lu, S. Q. (2008). Experimental study on suspended sediment distribution in flow with rigid vegetation, (Doctoral dissertation). Hohai University, Nanjing, Jiangsu, China (in Chinese).
- Moltchanov, S., Bohbot, R. Y., Duman, T., & Shavit, U. (2015). Canopy edge flow: A momentum balance analysis. *Water Resources Research*, 51(4), 2081-2095. <https://doi.org/10.1002/2014WR015397>
- Nepf, H. M. (1999). Drag, turbulence, and diffusion in flow through emergent vegetation. *Water Resources Research*, 2(35), 479-489. <https://doi.org/10.1029/1998WR900069>
- Nepf, H. M. (2004). Vegetated flow dynamics. In S. Fagherazzi, M. Marani, L. K. Blum (Eds.), *The Ecogeomorphology of Tidal Marshes* (Vol. 59, pp. 137-163). Washington, DC: American Geophysical Union. <https://doi.org/10.1029/CE059p0137>
- Nepf, H. M. (2012). Flow and transport in regions with aquatic vegetation. *Annual Review of Fluid Mechanics*, 44(1), 123-142. <https://doi.org/10.1146/annurev-fluid-120710-101048>
- Nepf, H. M., Sullivan, J. A., & Zavistoski, R. A. (1997). A model for diffusion within emergent vegetation. *Limnology and Oceanography*, 42(8), 1735-1745. <https://doi.org/10.4319/lo.1997.42.8.1735>
- Nepf, H. M., & Vivoni, E. R. (2000). Flow structure in depth-limited, vegetated flow. *Journal of Geophysical Research: Oceans*, 105(C12), 28547-28557. <https://doi.org/10.1029/2000jc900145>
- Nikora, V., McEwan, I., McLean, S., Coleman, S., Pokrajac, D., & Walters, R. (2007a). Double-averaging concept for rough-bed open-channel and overland flows: theoretical background. *Journal of Hydraulic Engineering*, 133(8), 873-883. [https://doi.org/10.1061/\(ASCE\)0733-9429\(2007\)133:8\(873\)](https://doi.org/10.1061/(ASCE)0733-9429(2007)133:8(873))
- Nikora, V., McLean, S., Coleman, S., Pokrajac, D., McEwan, I., & Campbell, L. (2007b). Double-averaging concept for rough-bed open-channel and overland flows: applications. *Journal of Hydraulic Engineering*, 133(8), 884-895. [https://doi.org/10.1061/\(ASCE\)0733-9429\(2007\)133:8\(884\)](https://doi.org/10.1061/(ASCE)0733-9429(2007)133:8(884))
- Poggi, D., & Katul, G. G. (2008a). Micro- and macro-dispersive fluxes in canopy flows. *Acta Geophysica*, 56(3), 778-799. <https://doi.org/10.2478/s11600-008-0029-7>
- Poggi, D., & Katul, G. G. (2008b). The effect of canopy roughness density on the constitutive components of the dispersive stresses. *Experiments in Fluids*, 45(1), 111-121. <https://doi.org/10.1007/s00348-008-0467-7>
- Poggi, D., Katul, G. G., & Albertson, J. D. (2004b). A note on the contribution of dispersive fluxes to momentum transfer within canopies. *Boundary-Layer Meteorology*, 111(3), 615-621. <https://doi.org/10.1023/b:boun.0000016563.76874.47>
- Poggi, D., Porporato, A., & Ridolfi, L. (2004a). The effect of vegetation density on canopy sub-layer turbulence. *Boundary-Layer Meteorology*, 111(3), 565-587. <https://doi.org/10.1023/b:boun.0000016576.05621.73>
- Raupach, M. R., Finnigan, J. J., & Brunei, Y. (1996). Coherent eddies and turbulence in vegetation canopies: The mixing-layer analogy. *Boundary-Layer Meteorology*, 78(3-4), 351-382. <https://doi.org/10.1007/BF00120941>

- Righetti, M. (2008). Flow analysis in a channel with flexible vegetation using double-averaging method. *Acta Geophysica*, 56(3), 801-823. <https://doi.org/10.2478/s11600-008-0032-z>
- Rouse, H. (1937). Modern conceptions of the mechanics of fluid turbulence. *Transactions of American Society of Civil Engineers*, 102, 463–505.
- Sonnenwald, F., Stovin, V., & Guymet, I. (2019). Estimating drag coefficient for arrays of rigid cylinders representing emergent vegetation. *Journal of Hydraulic Research*, 57(4), 591-597. <https://doi.org/10.1080/00221686.2018.1494050>
- Spiller, S. M., Rüther, N., & Baumann, B. (2015). Form-induced stress in non-uniform steady and unsteady open channel flow over a static rough bed. *International Journal of Sediment Research*, 30(4), 297-305. <http://dx.doi.org/10.1016/j.ijsrc.2014.10.002>
- Stoesser, T., & Nikora, V. I. (2008). Flow structure over square bars at intermediate submergence: Large Eddy Simulation study of bar spacing effect. *Acta Geophysica*, 56(3), 876-893. <https://doi.org/10.2478/s11600-008-0030-1>
- Tan, G. M., Fang, H. W., Dey, S., & Wu, W. M. (2018). Rui-jin zhang's research on sediment transport. *Journal of Hydraulic Engineering*, 144(6), 02518002.1-02518002.6. [https://doi.org/10.1061/\(ASCE\)HY.1943-7900.0001464](https://doi.org/10.1061/(ASCE)HY.1943-7900.0001464)
- Tanino, Y., & Nepf, H. M. (2008a). Lateral dispersion in random cylinder arrays at high Reynolds number. *Journal of Fluid Mechanics*, 600, 339-371. <https://doi.org/10.1017/S0022112008000505>
- Tanino, Y., & Nepf, H. M. (2008b). Laboratory investigation of mean drag in a random array of rigid, emergent cylinders. *Journal of Hydraulic Engineering*, 134(1), 34-41. [https://doi.org/10.1061/\(ASCE\)0733-9429\(2008\)134:1\(34\)](https://doi.org/10.1061/(ASCE)0733-9429(2008)134:1(34))
- Termini, D. (2019). Turbulent mixing and dispersion mechanisms over flexible and dense vegetation. *Acta Geophysica*, 67(3), 961-970. <https://doi.org/10.1007/s11600-019-00272-8>
- Tsai, C. W., & Huang, S. H. (2019). Modeling suspended sediment transport under influence of turbulence ejection and sweep events, *Water Resources Research*, 55(7), 5379-5393. <https://doi.org/10.1029/2018WR023493>
- van Rijn, L. C. (1984). Sediment transport, part II: suspended load transport. *Journal of Hydraulic Engineering*, 110(11), 1613-1641. [https://doi.org/10.1061/\(ASCE\)0733-9429\(1984\)110:11\(1613\)](https://doi.org/10.1061/(ASCE)0733-9429(1984)110:11(1613))
- Västilä, K., & Järvelä, J. (2018). Characterizing natural riparian vegetation for modeling of flow and suspended sediment transport. *Journal of Soils and Sediments*, 18(10), 3114-3130. <https://doi.org/10.1007/s1136>
- Wang, W., Huai, W. X., & Gao, M. (2014). Numerical investigation of flow through vegetated multi-stage compound channel. *Journal of Hydrodynamics*, 26(3), 467-473. [https://doi.org/10.1016/S1001-6058\(14\)60053-6](https://doi.org/10.1016/S1001-6058(14)60053-6)
- Wang, X. Y., Xie, W. M., Zhang, D., & He, Q. (2016). Wave and vegetation effects on flow and suspended sediment characteristics: A flume study. *Estuarine, Coastal and Shelf Science*, 182, 1-11. <http://dx.doi.org/10.1016/j.ecss.2016.09.009>

- Wilson, C. A. M. E. (2007). Flow resistance models for flexible submerged vegetation. *Journal of Hydrology*, 342(3-4), 213-222. <https://doi.org/10.1016/j.jhydrol.2007.04.022>
- Yang, J. Q., & Nepf, H. M. (2019), Impact of Vegetation on Bed Load Transport Rate and Bedform Characteristics, *Water Resources Research*, 55(7), 6109-6124. <https://doi.org/10.1029/2018WR024404>
- Yang, W., & Choi, S. (2010). A two-layer approach for depth-limited open-channel flows with submerged vegetation. *Journal of Hydraulic Research*, 48(4), 466-475. <https://doi.org/10.1080/00221686.2010.491649>
- Yuuki, T., & Okabe, T. (2002). Hydrodynamic mechanism of suspended load on riverbeds vegetated by woody plants. *Proceedings of Hydraulic Engineering*, 46, 701–706 (in Japanese). <https://doi.org/10.2208/prohe.46.701>
- Zhang, R. J., & Xie, J. H. (1989). River sediment dynamics (in Chinese). Beijing, CHN: China Water and Power Press. ISBN: 9787801244260.